



**HAL**  
open science

## Trends and drivers of anthropogenic NO emissions in China since 2020

Hui Li, Bo Zheng, Yu Lei, Didier Hauglustaine, Cuihong Chen, Xin Lin, Yi  
Zhang, Qiang Zhang, Kebin He

► **To cite this version:**

Hui Li, Bo Zheng, Yu Lei, Didier Hauglustaine, Cuihong Chen, et al.. Trends and drivers of anthropogenic NO emissions in China since 2020. *Environmental Science and Ecotechnology*, 2024, 21, pp.100425. 10.1016/j.esec.2024.100425 . hal-04621438

**HAL Id: hal-04621438**

**<https://hal.science/hal-04621438>**

Submitted on 24 Jun 2024

**HAL** is a multi-disciplinary open access archive for the deposit and dissemination of scientific research documents, whether they are published or not. The documents may come from teaching and research institutions in France or abroad, or from public or private research centers.

L'archive ouverte pluridisciplinaire **HAL**, est destinée au dépôt et à la diffusion de documents scientifiques de niveau recherche, publiés ou non, émanant des établissements d'enseignement et de recherche français ou étrangers, des laboratoires publics ou privés.



Contents lists available at ScienceDirect

# Environmental Science and Ecotechnology

journal homepage: [www.journals.elsevier.com/environmental-science-and-ecotechnology/](http://www.journals.elsevier.com/environmental-science-and-ecotechnology/)

Original Research

## Trends and drivers of anthropogenic NO<sub>x</sub> emissions in China since 2020



Hui Li <sup>a, b</sup>, Bo Zheng <sup>a, b, \*</sup>, Yu Lei <sup>c</sup>, Didier Hauglustaine <sup>d</sup>, Cuihong Chen <sup>e</sup>, Xin Lin <sup>d</sup>, Yi Zhang <sup>f</sup>, Qiang Zhang <sup>g</sup>, Kebin He <sup>b, h</sup>

<sup>a</sup> Shenzhen Key Laboratory of Ecological Remediation and Carbon Sequestration, Institute of Environment and Ecology, Tsinghua Shenzhen International Graduate School, Tsinghua University, Shenzhen 518055, China

<sup>b</sup> State Environmental Protection Key Laboratory of Sources and Control of Air Pollution Complex, Beijing 100084, China

<sup>c</sup> State Environmental Protection Key Laboratory of Environmental Planning and Policy Simulation and Center of Air Quality Simulation and System Analysis, Chinese Academy of Environmental Planning, Beijing 100041, China

<sup>d</sup> Laboratoire des Sciences du Climat et de l'Environnement, LSCE/IPSL, CEA-CNRS-UVSQ, Université Paris-Saclay, Gif-sur-Yvette, France

<sup>e</sup> Center for Satellite Application on Ecology and Environment, Ministry of Ecology and Environment of China, Beijing 100094, China

<sup>f</sup> Institute of Future Human Habitats, Tsinghua Shenzhen International Graduate School, Tsinghua University, Shenzhen 518055, China

<sup>g</sup> Ministry of Education Key Laboratory for Earth System Modeling, Department of Earth System Science, Tsinghua University, Beijing 100084, China

<sup>h</sup> State Key Joint Laboratory of Environment Simulation and Pollution Control, School of Environment, Tsinghua University, Beijing 100084, China

### ARTICLE INFO

#### Article history:

Received 8 November 2023

Received in revised form

19 April 2024

Accepted 20 April 2024

#### Keywords:

China's NO<sub>x</sub> emissions

Pollution control

Socio-economic drivers

Atmospheric inversion

### ABSTRACT

Nitrogen oxides (NO<sub>x</sub>), significant contributors to air pollution and climate change, form aerosols and ozone in the atmosphere. Accurate, timely, and transparent information on NO<sub>x</sub> emissions is essential for decision-making to mitigate both haze and ozone pollution. However, a comprehensive understanding of the trends and drivers behind anthropogenic NO<sub>x</sub> emissions from China—the world's largest emitter—has been lacking since 2020 due to delays in emissions reporting. Here we show a consistent decline in China's NO<sub>x</sub> emissions from 2020 to 2022, despite increased fossil fuel consumption, utilizing satellite observations as constraints for NO<sub>x</sub> emission estimates through atmospheric inversion. This reduction is corroborated by data from two independent spaceborne instruments: the Tropospheric Monitoring Instrument (TROPOMI) and the Ozone Monitoring Instrument (OMI). Notably, a reduction in transport emissions, largely due to the COVID-19 lockdowns, slightly decreased China's NO<sub>x</sub> emissions in 2020. In subsequent years, 2021 and 2022, reductions in NO<sub>x</sub> emissions were driven by the industry and transport sectors, influenced by stringent air pollution controls. The satellite-based inversion system developed in this study represents a significant advancement in the real-time monitoring of regional air pollution emissions from space.

© 2024 The Authors. Published by Elsevier B.V. on behalf of Chinese Society for Environmental Sciences, Harbin Institute of Technology, Chinese Research Academy of Environmental Sciences. This is an open access article under the CC BY license (<http://creativecommons.org/licenses/by/4.0/>).

### 1. Introduction

Nitrogen oxides (NO<sub>x</sub> = NO + NO<sub>2</sub>), an active and short-lived air pollutant, have been well-known for their crucial role in ozone photochemistry [1], haze chemistry [2], and climate impacts [3]. The emissions of NO<sub>x</sub> contribute to the formation of acid rain [4], O<sub>3</sub> pollution [5], and haze pollution [6], leading to air pollution-related

deaths [7] and damage to ecosystems. China is the largest emitter of NO<sub>x</sub> at present, accounting for about 24% of the global total at present (<https://edgar.jrc.ec.europa.eu/>) [8]. Recognizing the NO<sub>x</sub>-induced environmental issues, China has been reinforcing the control of NO<sub>x</sub> emissions from anthropogenic sources, especially since 2013, when severe haze attracted broad attention and triggered the toughest-ever air pollution control actions [9].

The major sources of NO<sub>x</sub> emissions are fossil fuel consumption in power generation [10–12], transportation [13], iron and steel production [14], and cement production [15]. China has enforced ultra-low emission standards for coal-fired power plants [16,17] as well as cement and iron production [18]. Emission standards for on-road vehicles have been progressively upgraded from China III to

\* Corresponding author. Shenzhen Key Laboratory of Ecological Remediation and Carbon Sequestration, Institute of Environment and Ecology, Tsinghua Shenzhen International Graduate School, Tsinghua University, Shenzhen 518055, China.

E-mail address: [bozheng@sz.tsinghua.edu.cn](mailto:bozheng@sz.tsinghua.edu.cn) (B. Zheng).

China VI from 2017 to 2023, imposing stricter limits on NO<sub>x</sub> emissions standards from 150 to 60 mg km<sup>-1</sup> [19]. Measures have also been taken to phase out small or outdated industrial capacities, coal-fired power plants, and old “yellow-labeled” vehicles. These efforts together have led to a steady decline in China’s NO<sub>x</sub> emissions since 2012, with the industry, transport, and power sectors as primary contributors [13,20,21].

Since 2020, the world has experienced drastic socio-economic changes, including global economic inflation [22], pandemic prevention measures [23], and initiatives toward carbon neutrality [24], which have incurred widespread and substantial changes in human activities. These socio-economic changes have introduced substantial challenges in evaluating anthropogenic emission changes timely and the associated impacts on the atmospheric environment. The conventional bottom-up approach, based on activity data and emission factors, is limited by the availability of timely and accurate data [25]. The top-down method, using atmospheric observation constraints to infer emissions, can circumvent the dilemma of data availability, as most observational data and meteorological reanalysis fields are publicly accessible and updated in near real-time [26,27]. Satellite-based monitoring has become a widely used tool for NO<sub>x</sub> emission estimation, benefiting from its large signal-to-noise ratio, broad spatial coverage and high spatial resolution, and continuous temporal availability [28–31].

A decline in anthropogenic NO<sub>x</sub> emissions was temporally observed in 2020, driven by the strict quarantine measures [32]. However, we currently lack a complete understanding of the changes and drivers of China’s anthropogenic NO<sub>x</sub> emissions after 2020. To bridge the data gap, we utilize our previously developed and well-validated atmospheric inversion system based on satellite observations [33,34] to estimate the monthly and sectoral NO<sub>x</sub> emissions in the Chinese mainland from 2020 to 2022. To confirm the robustness of our results, we utilize Tropospheric Monitoring Instrument (TROPOMI) and Ozone Monitoring Instrument (OMI) satellite NO<sub>2</sub> retrievals as observational constraints in our inversions, respectively, as mutual verification. China’s anthropogenic NO<sub>x</sub> emissions by month, sector, and province are then further investigated in detail to resolve the drivers of emission variations, including air pollution control and socio-economic factor changes.

## 2. Materials and methods

### 2.1. Satellite NO<sub>2</sub> retrievals

TROPOMI, on board the European Copernicus Sentinel-5 Precursor (S5P) launched in October 2017 [35], is the most widely used satellite instrument monitoring NO<sub>2</sub> pollution because it offers global daily NO<sub>2</sub> tropospheric vertical column densities (TVCDs) sampled at 13:30 local time with a current resolution of up to 5.5 × 3.5 km [36]. Here we used version 2.4.0 of TROPOMI NO<sub>2</sub> TVCDs as the observational constraint in inversion ([https://www.temis.nl/airpollution/no2col/no2regio\\_tropomi.php](https://www.temis.nl/airpollution/no2col/no2regio_tropomi.php)), which could reduce the low-biased errors of the previous data versions [37]. To evaluate our results, we also employed OMI NO<sub>2</sub> retrievals version 3 [38] as observational constraints in our inversion separately. OMI is on the National Aeronautics and Space Administration (NASA)’s EOS-Aura spacecraft, providing global daily NO<sub>2</sub> TVCDs sampled at 13:40 local time with a resolution of 13 × 24 km ([https://aura.gesdisc.eosdis.nasa.gov/data/Aura\\_OMI\\_Level2/OMNO2.003/](https://aura.gesdisc.eosdis.nasa.gov/data/Aura_OMI_Level2/OMNO2.003/)) [39]. We filtered out the data of poor quality for TROPOMI and OMI [40] and mapped the NO<sub>2</sub> TVCDs at a resolution of 0.5° × 0.625° to match the horizontal resolution of our chemical transport model [33]. Our analysis only retained the grid cells dominated by anthropogenic NO<sub>x</sub> emissions, where the daily NO<sub>2</sub> TVCDs

exceeded 1 × 10<sup>15</sup> molecules cm<sup>-2</sup> [41].

### 2.2. Prior NO<sub>x</sub> emissions

We used the bottom-up approach to estimate China’s NO<sub>x</sub> emissions between 2020 and 2022 as prior, based on the MEIC (Multi-resolution Emission Inventory for China) emission inventory in 2019 and the year-on-year monthly changes in activity levels from 2019 to the target years (i.e., 2020, 2021, and 2022) [32]. The monthly changes in thermal power generation, cement production, iron production, and manufacturing value added from the National Bureau of Statistics (<http://www.stats.gov.cn/>) were used to infer the changes in activity levels of the power, cement, iron, and other industries, respectively. To account for January and February separately, combined in official statistical reports, we utilized the production index to differentiate the activity levels between these two months. Regarding the transport sector, we employed monthly changes in on-road freight turnover and construction area to represent the changes in emissions from the on- and off-road sectors. The changes in the freight turnover served as a good proxy for heavy-duty truck activities, which accounted for a majority of transport NO<sub>x</sub> emissions in China [42]. For the residential heating emissions, the provincial population-weighted heating degree days were used to represent the monthly changes in activity levels of heating boilers and stoves, except for provinces located on the same latitude band as Guangdong and those to the south (i.e., Guangdong, Guangxi, and Hainan provinces), where residential stoves were rarely used. The residential heating NO<sub>x</sub> emissions were low and assumed unchanged since 2019 [34].

### 2.3. Inversion estimation of sectoral NO<sub>x</sub> emissions

The monthly total NO<sub>x</sub> emissions between 2020 and 2022 in China were inferred from satellite retrievals of NO<sub>2</sub> TVCDs using the mass balance method [43], assuming a localized relation between the changes in NO<sub>2</sub> TVCDs and NO<sub>x</sub> emissions.

$$E_{t,i,\text{sate},y} = \left( 1 + \beta_{t,i} \left( \frac{\Delta Q}{Q} \right)_{t,i,\text{anth},y} \right) \times E_{t,i,\text{bottom-up},2019} \quad (1)$$

$$\left( \frac{\Delta Q}{Q} \right)_{t,i,\text{anth},y} = \frac{Q_{t,i,\text{sate},y}}{Q_{t,i,\text{sate},2019}} - \frac{Q_{t,i,\text{simu\_fixemis},y}}{Q_{t,i,\text{simu},2019}} \quad (2)$$

In these equations,  $t$ ,  $i$ , and  $y$  represent the month, grid cell (i.e., 0.5° × 0.625°), and year (i.e., 2020, 2021, and 2022), respectively.  $E_{t,i,\text{sate},y}$  is the anthropogenic NO<sub>x</sub> emissions constrained by satellite NO<sub>2</sub> TVCDs (i.e., TROPOMI or OMI).  $E_{t,i,\text{bottom-up},2019}$  is the anthropogenic NO<sub>x</sub> emissions in 2019 from the MEIC model.  $\beta_{t,i}$  is a unitless factor relating the changes in NO<sub>2</sub> TVCDs to the changes in anthropogenic NO<sub>x</sub> emissions [44], acquired by a perturbation (i.e., -40%) of China’s anthropogenic NO<sub>x</sub> emissions in 2019 (details in Materials and Methods in the Supplementary Information (SI)). For abnormal occurrences of  $\beta_{t,i}$ , specifically when  $\beta_{t,i}$  exceeds 2, we masked those grids to mitigate the influence of these anomalies on the results.  $\left( \frac{\Delta Q}{Q} \right)_{t,i,\text{anth},y}$  refers to the relative changes in satellite NO<sub>2</sub> TVCDs ( $Q$ ) due to anthropogenic NO<sub>x</sub> emissions from 2019 to year  $y$ .  $\frac{Q_{t,i,\text{sate},y}}{Q_{t,i,\text{sate},2019}}$  indicates the relative differences in satellite NO<sub>2</sub> TVCDs, and  $\frac{Q_{t,i,\text{simu\_fixemis},y}}{Q_{t,i,\text{simu},2019}}$  represents the relative differences in NO<sub>2</sub> TVCDs caused by meteorological fluctuations, estimated by GEOS-Chem model simulations with the fixed 2019 emissions and meteorological field in year  $y$ . We used GEOS-Chem 12.3.0 (<https://geoschem.github.io/>) driven by the meteorological fields from the MERRA-2 Reanalysis of the NASA Global Modeling and Assimilation

Office [45]. Details on the inversion method and model settings can be found in our previous work (Materials and Methods in SI) [33,34]. While the GEOS-Chem simulated NO<sub>2</sub> TVCDs exhibit a low bias compared to the TROPOMI observation, their spatial distribution and annual means are in strong agreement (Fig. S1). Furthermore, adopting relative changes in either the simulated NO<sub>2</sub> TVCDs or TROPOMI observational NO<sub>2</sub> TVCDs (equation (2)) can alleviate the influence of the low bias in absolute NO<sub>2</sub> TVCDs on emission estimates.

The monthly NO<sub>x</sub> emissions were attributed to each source sector by integrating the prior information on sectoral emission spatial distributions. We summarized the difference between inversion and prior emission estimates in grid cells dominated by each source sector, whose contribution exceeded 50% of the grid's total emissions in prior. These discrepancies were used to derive scaling factors for each source sector and correct the prior NO<sub>x</sub> emissions by sector. The corrected prior emissions were finally rescaled to ensure consistency with the satellite-constrained NO<sub>x</sub> emissions for national totals. Details for sectoral emission estimation can be found in our previous studies (Materials and Methods in SI) [33,34]. The good correlation observed between GEOS-Chem simulated and TROPOMI observational NO<sub>2</sub> TVCDs (Fig. S1), along with the correlation between GEOS-Chem simulated and ground station monitored surface NO<sub>2</sub> concentrations (<http://www.cnemc.cn/>) (Fig. S2), attests to the robustness and reliability of our NO<sub>x</sub> emission estimations.

### 3. Results and discussion

#### 3.1. Decline in China's NO<sub>x</sub> emissions since 2020

Our inversions reveal that China's NO<sub>x</sub> emissions have declined since 2020, with a progressively steeper rate of decrease (black curves in Fig. 1). The year-on-year reductions in China's NO<sub>x</sub> emissions, as monitored by the TROPOMI satellite, were 2.7% in 2020, 3.5% in 2021, and 7.6% in 2022 (Fig. 1a), which align with the OMI-constrained inversion (dashed curves in Fig. 1c and d). China's NO<sub>x</sub> emissions are estimated to have declined by 10.8% from 2020 to 2022, which is consistent with the surface NO<sub>2</sub> concentrations measured by ground stations in China (down by 12.5% from 2020 to 2022) (details refer to Section 1.7 in Materials and Methods in SI). Besides, we utilize the TROPOMI-constrained NO<sub>x</sub> emissions to drive the global chemical transport model (LMDZ-INCA) used by Peng et al. [46]. The simulated NO<sub>2</sub> TVCDs based on LMDZ-INCA closely replicate the annual variations observed by TROPOMI (deep orange line in Fig. S3b). The broad consistency of multiple lines of evidence confirms the rapid drop in China's NO<sub>x</sub> emissions since 2020. Unless stated separately, the inversion NO<sub>x</sub> emissions in the following text refer to the TROPOMI-based estimates.

Industrial production, energy use, and CO<sub>2</sub> emissions in China did not decline as the inversion-based NO<sub>x</sub> emissions but increased moderately since 2020 (Fig. 1b–d). The thermal power generation and industry value added grew annually by 0.9–8.4% and 2.8–9.6%, respectively, between 2020 and 2022. The freight turnover decreased by 1.0% in 2020 but rebounded by 10.9% in 2021 and 3.4% in 2022, corresponding to rapid economic growth. Heavy industries in China showed fluctuations in their annual production, with iron and cement production rising in 2020 but dipping in 2021 and 2022. The total consumption of fossil fuels in China, including coal, oil, and natural gas, slightly decreased in 2020 by 0.3% but kept increasing since 2021, with growth rates of 6.0% in 2021 and 1.9% in 2022. China's CO<sub>2</sub> emissions, averaged between Carbon Monitor [47] and International Energy Agency (IEA 2023, <https://www.iea.org/>) estimates, increased by 0.7% and 6.0% in 2020 and 2021, respectively, and decreased slightly by 0.9% in 2022 (grey solid

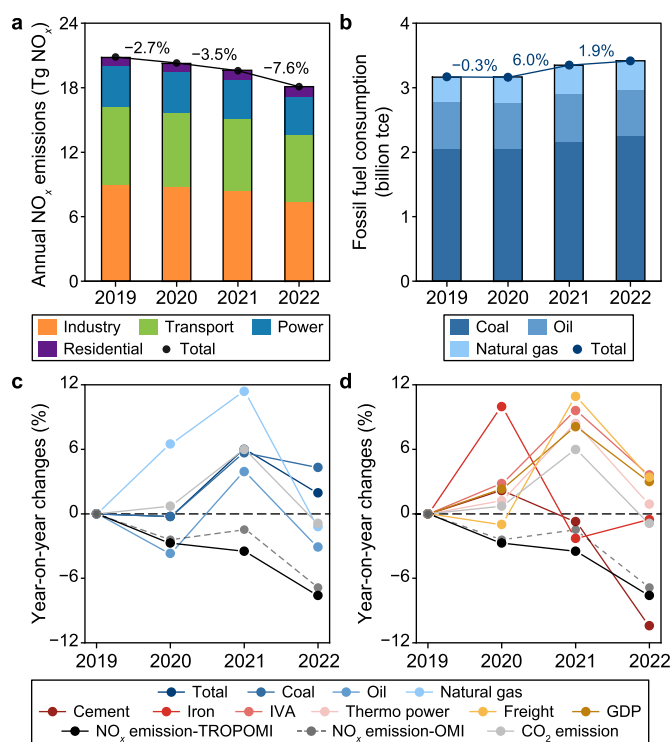


**Fig. 1.** Changes in TROPOMI-constrained annual NO<sub>x</sub> emissions, fossil fuel consumption, and main anthropogenic activities between 2020 and 2022. **a**, The changes in annual NO<sub>x</sub> emissions between 2020 and 2022. **b**, The annual changes in fossil fuel consumption between 2020 and 2022, including coal, oil, and natural gas. **c**, Year-on-year changes in fossil fuel consumption, NO<sub>x</sub> and CO<sub>2</sub> emissions between 2020 and 2022. **d**, Year-on-year changes in social-economic activities (<http://www.stats.gov.cn/>), NO<sub>x</sub>, and CO<sub>2</sub> emissions between 2020 and 2022. The changes in CO<sub>2</sub> emissions here are the averages of the estimates from Carbon Monitor (<https://cn.carbonmonitor.org/>) and IEA (<https://www.iea.org/>). Fossil fuel consumption refers solely to the quantity consumed through combustion. IVA: industry value added.

curves in Fig. 1c and d).

The discrepancy between NO<sub>x</sub> and CO<sub>2</sub> emission variations since 2020 reflects the divergent changes in the source sectors with different NO<sub>x</sub>-to-CO<sub>2</sub> emission ratios or the influences from NO<sub>x</sub> pollution control. To disentangle the possible drivers, we estimate China's NO<sub>x</sub> emissions by combining the sectoral NO<sub>x</sub> emissions in 2019 from MEIC with the annual percentage changes in sectoral CO<sub>2</sub> emissions since 2019 from Carbon Monitor (Fig. S3a). We further utilize such simply updated NO<sub>x</sub> emissions (refer to Carbon Monitor-based NO<sub>x</sub> emissions hereinafter) to drive the LMDZ-INCA model [46]. This simulated NO<sub>2</sub> TVCDs presented a 3.6% decline over China in 2020 compared to 2019, consistent with the TROPOMI observations (Fig. S3b). The Carbon Monitor-based NO<sub>x</sub> emissions reduction in 2020 agrees with our inversion results, in contrast to the slight growth of Carbon Monitor's CO<sub>2</sub> emissions. This suggests that the sectors with large NO<sub>x</sub>-to-CO<sub>2</sub> emission ratios decreased their emissions while the others increased emissions, causing an opposite change in total NO<sub>x</sub> and CO<sub>2</sub> emissions in 2020. The transport sector has the largest NO<sub>x</sub>-to-CO<sub>2</sub> emission ratio in China (0.008, 0.002, 0.001, and 0.001 for transport, industry, power, and residential sectors according to the 2019 MEIC emission inventory) [13]. Their emissions possibly dropped in 2020, as reflected by the reduction in oil consumption (Fig. 1c, Fig. S4, Tables S1 and S2) and freight turnover (Fig. 1d).

The NO<sub>x</sub> emissions from the Carbon Monitor-based estimates increase by 7.6% in 2021 and decrease by 3.0% in 2022, which are close to the Carbon Monitor CO<sub>2</sub> emission changes, while our

inversion-based  $\text{NO}_x$  emissions show substantial declines (Fig. S3a). The atmospheric simulation of LMDZ-INCA driven by the Carbon Monitor-based  $\text{NO}_x$  emissions shows a 5.3% increase in  $\text{NO}_2$  TVCDs over China in 2021, while TROPOMI and OMI observations reveal a decrease of 3.9% and 2.1%, respectively, suggesting that China's  $\text{NO}_x$  emissions did not rebound like  $\text{CO}_2$  emissions (Fig. S3b). Although the changes in activity levels of different source sectors tend to result in concurrent interannual variations of  $\text{NO}_x$  and  $\text{CO}_2$  emissions, the other factors, most likely the  $\text{NO}_x$  pollution control related to clean air actions, drive down  $\text{NO}_x$  emissions fast.

### 3.2. Drivers of $\text{NO}_x$ emissions decline in China

We break out the annual reductions in inversion-based  $\text{NO}_x$  emissions since 2020 by quarter (Fig. 2a) and by source sector (Fig. 2b) to illustrate the socio-economic drivers. Our inversion constrained by OMI observations (Fig. S5) provides consistent results as TROPOMI. In 2020, the analysis of emission variation by quarter and sector suggests that China's  $\text{NO}_x$  emissions declined in the first quarter (Q1) while rebounded in the remaining three-quarters (Fig. 2a). This is mainly due to the stringent lockdown response to the first wave of the Coronavirus Disease 2019 (COVID-19) pandemic in China lasting from January 23 to April 7 in 2020 and the rapid emissions rebound after that when the lockdown restriction lifted [33,48]. The transport sector, which was largely influenced by the COVID-19 lockdown, accounted for two-thirds of the annual emissions decline in 2020 (Fig. 2b). Besides, the transition from traditional vehicles to electric cars, promoted by the Chinese government, has further contributed to the reduction of  $\text{NO}_x$  emissions in the transport sector [49]. This is consistent with

our analysis, which identifies the sector with large  $\text{NO}_x$ -to- $\text{CO}_2$  emission ratios as one of the main factors driving down China's  $\text{NO}_x$  emissions in 2020.

In 2021 and 2022, China's  $\text{NO}_x$  emissions declined in all quarters except Q1 2021, compared to the corresponding quarter of the year before (Fig. 2a). The emissions increase in Q1 2021 is because of the lockdown-induced emissions drop in Q1 2020. The industry sector primarily dominated the emissions decline in 2021, while the industry and transport sectors both drove the decline in 2022 (Fig. 2b). The  $\text{NO}_x$  pollution control in these two sectors is probably the main driver of the decline in emissions. China had completed the ultra-low emission retrofitting for 145 million tons and 250 million tons of steel production capacity, respectively, as of 2021 and 2022. Pollution control endeavors were also pursued in the cement, coke, and petrochemical industries ([https://www.mee.gov.cn/ywtd/zbf/202303/t20230328\\_1022381.shtml](https://www.mee.gov.cn/ywtd/zbf/202303/t20230328_1022381.shtml)). The transport sector has seen the enforcement of stricter vehicle emission standards, such as the China VI standard for light-duty vehicles that commenced in 2020 [50]. In 2021 and 2022, there was a total elimination of 4.2 million ([https://www.mee.gov.cn/ywtd/hjywnews/202204/t20220421\\_975549.shtml](https://www.mee.gov.cn/ywtd/hjywnews/202204/t20220421_975549.shtml)) and 6.2 million ([https://www.mee.gov.cn/ywtd/zbf/202303/t20230328\\_1022381.shtml](https://www.mee.gov.cn/ywtd/zbf/202303/t20230328_1022381.shtml)) polluted and old vehicles, respectively.

Other factors, such as the structural change in China's economy and the COVID-19 influences, also contributed to the steady decline in  $\text{NO}_x$  emissions in 2021 and 2022. For example, the substantial decreases of  $\text{NO}_x$  emissions in the third quarter (Q3) and fourth quarter (Q4) of 2021 were concurrent with the drop in cement and iron production (Fig. S6), possibly due to the tightened regulation for the real estate sector since July 2021 (<https://www.mohurd.gov.cn/>). The  $\text{NO}_x$  emissions decline in 2022 mainly occurred in the second quarter (Q2) and Q4, when cement production declined by 16.7% and 5.1%, respectively, and the on-road freight turnover decreased by 1.3% and 2.5%, respectively. The emission decreases also coincided with the diminished economic activities due to the Omicron-incurred lockdown in Q2 [51] and the nationwide optimization of the COVID-19 policies at the end of 2022 (<https://www.gov.cn/>). Still, as shown in Section 3.1, air pollution control measures dominated China's  $\text{NO}_x$  emissions cut in 2021 and 2022.

### 3.3. $\text{NO}_x$ emission changes and drivers by province

The changes in China's  $\text{NO}_x$  emissions since 2020 vary by province and present broad spatial heterogeneity (Fig. 3a, Fig. S7), as well as uneven distribution of emissions and  $\text{NO}_2$  TVCDs (Figs. S7–S9). In 2020, when COVID-19 started to hit China, a majority of China's provinces observed a decline in both fossil fuel consumption and inversed  $\text{NO}_x$  emissions compared to those in 2019 (Fig. 3b). The impacts of the COVID-19 lockdowns on industry and transport sectors led to substantial emission reductions in the provinces with high industrialization levels and dense populations (Fig. S10). The provinces with large emission reductions were mostly located around Hubei, which experienced stringent lockdowns (Fig. S7a). For instance, Hubei, Shanghai, and Jiangsu witnessed  $\text{NO}_x$  emission reductions of 4.3%, 15.1%, and 8.7%, respectively. In contrast, Heilongjiang, Jilin, and Liaoning, the provinces in Northeast China that are geographically distant from Hubei, observed increases in  $\text{NO}_x$  emissions by 7.6%, 7.1%, and 2.0%, respectively, in 2020 (Fig. 3a, Fig. S7a). This rise in  $\text{NO}_x$  emission in these provinces aligns with their increase in industrial production. Taking industry value added as an example, there was a notable upswing of 3.3%, 6.9%, and 1.8% in Heilongjiang, Jilin, and Liaoning, respectively.

Since 2021,  $\text{NO}_x$  emissions have declined remarkably in most of China's provinces (Fig. 3a, Figs. S7b and c), despite the increased

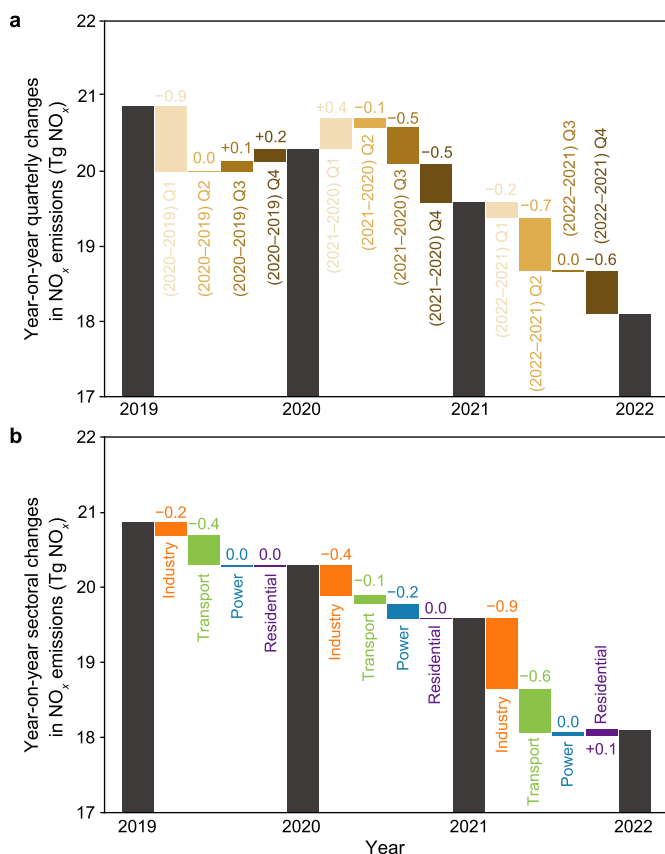
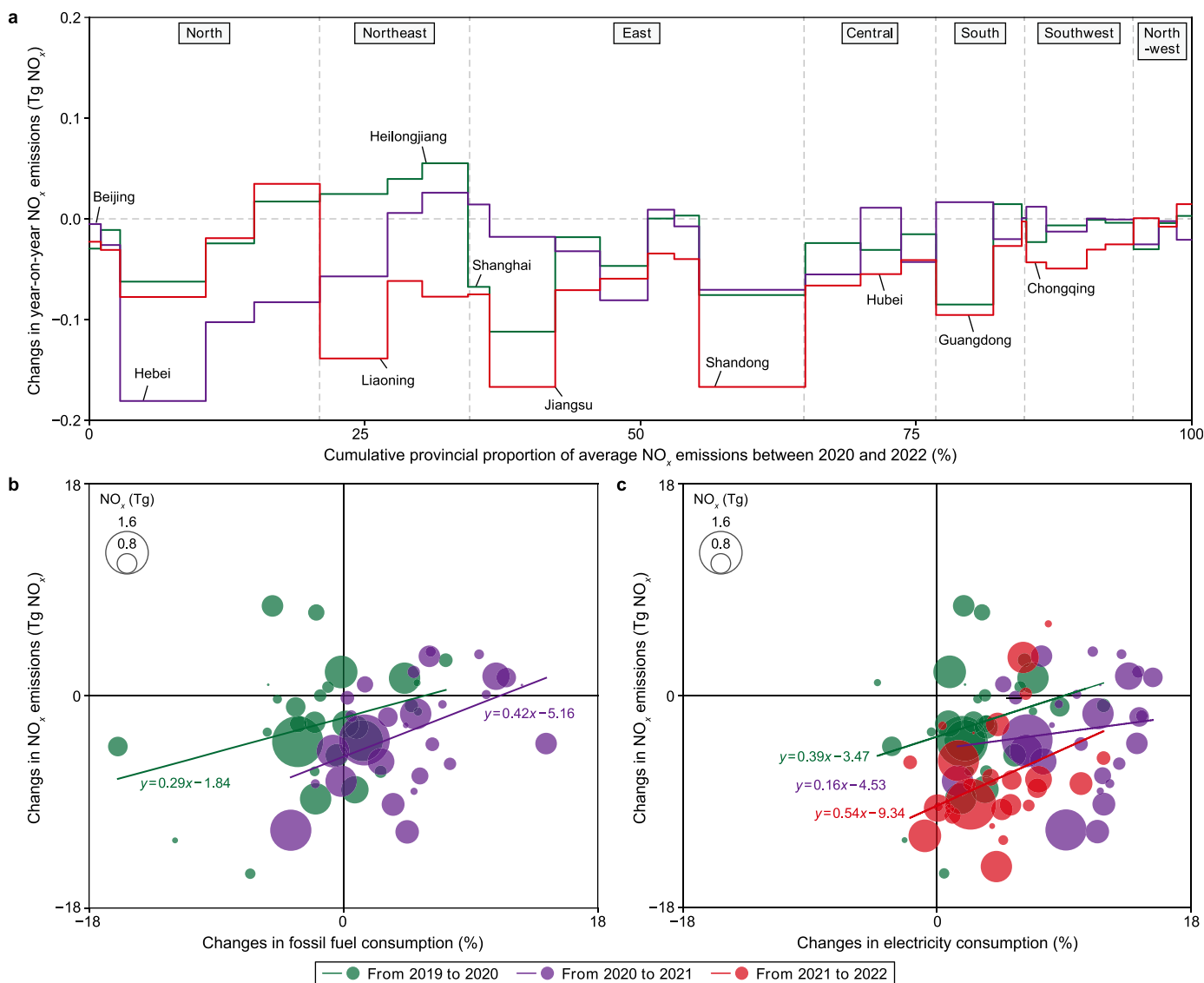


Fig. 2. Year-on-year  $\text{NO}_x$  emission variations by quarter (a) and sector (b) between 2020 and 2022.



**Fig. 3.** Provincial contribution to the year-on-year NO<sub>x</sub> emission changes in China between 2020 and 2022. **a**, Provincial contribution to the year-on-year NO<sub>x</sub> emission changes between 2019 and 2022 (region classification is introduced in Table S3). **b**, Correlations between the changes in provincial NO<sub>x</sub> emissions and provincial fossil fuel consumption (refers only to the quantity consumed through combustion). Due to the unavailability of provincial fossil fuel consumption data for 2022, this panel only presents data from 2019 to 2020 and 2020 to 2021. **c**, Correlations between the changes in provincial NO<sub>x</sub> emissions and provincial electricity consumption. The size of the dots refers to the provincial NO<sub>x</sub> emissions.

consumption of fossil fuel (Fig. 3b) and electricity (Fig. 3c), which reflects the nationwide efficacy of NO<sub>x</sub> pollution control measures. Seasonal fluctuations in industrial production and the COVID-19 impacts further shaped different changes in NO<sub>x</sub> emissions across provinces, modulated by the economic structure of each province. For example, in the latter half of 2021, iron production in Hebei — the province accounting for approximately one-quarter of China's total iron production — decreased by 17.5% compared to the corresponding period in 2020, which contributed to the 11.4% decline in Hebei's NO<sub>x</sub> emissions in 2021 compared to those in 2020. Conversely, the provinces whose economic structure is dominated by the service industry, finance, and vehicle manufacturing, such as Shanghai, Guangdong, and Chongqing, increased NO<sub>x</sub> emissions in 2021 due to the rebound in economic growth with few COVID-19 impacts.

In 2022, provinces with high levels of industrialization and

populations reduced NO<sub>x</sub> emissions substantially (Figs. S7c and S10), reflecting the combined impacts of air pollution control and socio-economic factor changes. Shanghai, Jiangsu, and Chongqing emerged as the top three provinces with the greatest NO<sub>x</sub> emissions decline, down by 19.0%, 14.5%, and 12.3%, respectively. These developed, densely-populated regions were typically influenced more by the COVID-19 Omicron wave in 2022, and their emissions were slashed by lockdowns [52,53]. On the contrary, the provinces with fewer population densities in North and Northwest China increased emissions in 2022 (Fig. 3a, Fig. S7c), including Ningxia (+6.1%), Nei Mongol (+3.3%), and Shaanxi (+0.2%). Overall, the relationship between changes in provincial NO<sub>x</sub> emissions and its economic structure was similar in 2020 and 2022, the two years with widespread COVID-19 lockdowns, suggesting consistent pandemic impacts on provincial NO<sub>x</sub> emissions (Fig. S10).

### 3.4. Uncertainty and limitation

The primary source of uncertainty in our NO<sub>x</sub> emission estimation arises from systematic and random errors associated with satellite NO<sub>2</sub> retrievals [54], simulated NO<sub>2</sub> columns from the GEOS-Chem model [55], and the inversion algorithm. While these errors may be inevitable, we have taken measures to minimize their potential influence on our conclusions as much as possible. To reduce systematic error influences stemming from satellite data, we employ relative changes in satellite NO<sub>2</sub> as observational constraints in the inference of the total NO<sub>x</sub> emission changes across different years, as indicated in equation (1). Likewise, we establish the relationship between the relative changes in NO<sub>x</sub> emissions and NO<sub>2</sub> columns ( $\beta$ ) using the GEOS-Chem model, thereby reducing systematic errors stemming from the model simulations. Above all, our findings are based on spatial and sectoral aggregations to decrease random errors associated with the estimation process and the data used. Our previous studies have shown the insensitivity of estimated emissions to crucial parameters like  $\beta$  in the inversion algorithm, demonstrating the inversion results' robustness [33,34]. The NO<sub>x</sub> emissions constrained by TROPOMI and OMI satellites exhibit comparable emission estimates since 2020, confirming the reliability of our results. Besides, the LMDZ-INCA simulated NO<sub>2</sub> TVCDs using our inversion-based NO<sub>x</sub> emissions closely match the interannual variations observed by satellites (deep orange line in Fig. S3), underscoring the reliability of the key findings in this study.

However, our methodology has certain limitations that warrant future improvements. First, we have simplified the nonlinear relationship between NO<sub>x</sub> emissions and NO<sub>2</sub> TVCDs and have not considered the inter-grid transport of NO<sub>2</sub>, using a linear relationship ( $\beta$ ) in the current inversion system on a grid-by-grid (resolution of  $0.5^\circ \times 0.625^\circ$ ) and month-by-month base. This assumption of approximate linearity and locality between NO<sub>x</sub> emissions and NO<sub>2</sub> TVCDs may introduce uncertainties, particularly during colder months when the NO<sub>2</sub> lifetime is extended [56]. Second, the horizontal resolution affects the establishment of localized links between them, as grids with excessively fine resolution pose challenges related to inter-grid transport, while grids with overly coarse resolution hinder the attribution of sectoral emissions [57], necessitating a more agile and appropriate selection. Third, our focus is solely on anthropogenic NO<sub>x</sub> emissions within grids where daily NO<sub>2</sub> TVCDs exceed  $1 \times 10^{15}$  molecules cm<sup>-2</sup>, irrespective of the influence of specific events like wildfires [41]. While few wildfire emissions are compared to anthropogenic sources in China, exercising caution and proactively identifying specific regions affected by such events is essential. This precautionary measure is necessary to mitigate the potential impact of the increasingly frequent wildfires expected in the future due to climate change [58,59].

## 4. Conclusions

This study reveals a steady decline in China's NO<sub>x</sub> emissions from 2020 to 2022, marking a reduction of 2.7% in 2020, 3.5% in 2021, and 7.6% in 2022, as confirmed by satellite-based atmospheric inversions. The reduced transport emissions, mainly due to the COVID-19 lockdown, led to the NO<sub>x</sub> emissions decline in 2020 and contributed 68.9% to the overall reduction. The industry and transport sectors drove down China's NO<sub>x</sub> emissions in 2021 and 2022 on a larger scale, which accounted for over 70% of the total reduction, possibly caused by air pollution control, as per our information. This study examines the encouraging outcome of China's ongoing clean air measures, which offers a viable blueprint for other countries grappling with their air quality challenges. It is noteworthy that, in the context of this study revealing the driving

force of pollution control in reducing NO<sub>x</sub> emissions, the rapid rebound in China's NO<sub>2</sub> concentration in early 2023, as we previously disclosed, further confirms the rapid resurgence of economic and human activities over a relatively short period can still offset the effects of air pollution control temporarily [40]. Despite a decrease in NO<sub>x</sub> emissions, we have not observed a concurrent decline in China's CO<sub>2</sub> emissions due to the increased fossil fuel consumption, which suggests a difficulty in achieving coordinated governance of air quality and climate pollutants under the current energy structure. We need effective tools to explore and support the energy, climate, and air quality policy synergies. The satellite-based inversion system present in this study could be a crucial part of such a system, enabling tracking air pollutant emissions by sector with low latency.

### CRedit authorship contribution statement

**Hui Li:** Formal Analysis, Investigation, Methodology, Software, Visualization, Writing - Original Draft, Writing - Review & Editing. **Bo Zheng:** Conceptualization, Funding Acquisition, Investigation, Methodology, Project Administration, Supervision, Writing - Review & Editing. **Yu Lei:** Writing - Review & Editing. **Didier Hauglustaine:** Software, Writing - Review & Editing. **Cuihong Chen:** Investigation. **Xin Lin:** Software, Writing - Review & Editing. **Yi Zhang:** Writing - Review & Editing. **Qiang Zhang:** Supervision, Writing - Review & Editing. **Kebin He:** Supervision, Writing - Review & Editing.

### Declaration of competing interest

The authors declare that they have no known competing financial interests or personal relationships that could have appeared to influence the work reported in this paper.

### Acknowledgments

This work was supported by the National Key R&D Program of China (Grant No. 2021YFB3901000), the National Natural Science Foundation of China (Grant No. 42105094), and the Shenzhen Science, Technology and Innovation Commission (Grant No. WDZC20220810110301001).

### Appendix A. Supplementary data

Supplementary data to this article can be found online at <https://doi.org/10.1016/j.ese.2024.100425>.

### References

- [1] R. Dang, D.J. Jacob, V. Shah, et al., Background nitrogen dioxide (NO<sub>2</sub>) over the United States and its implications for satellite observations and trends: effects of nitrate photolysis, aircraft, and open fires, *Atmos. Chem. Phys.* 23 (2023) 6271–6284.
- [2] Y. Cheng, G. Zheng, C. Wei, et al., Reactive nitrogen chemistry in aerosol water as a source of sulfate during haze events in China, *Sci. Adv.* 2 (2016) e1601530.
- [3] A. Skowron, D.S. Lee, R.R. De León, et al., Greater fuel efficiency is potentially preferable to reducing NO<sub>x</sub> emissions for aviation's climate impacts, *Nat. Commun.* 12 (2021) 564.
- [4] S. Zhao, S. Liu, X. Hou, et al., Temporal dynamics of SO<sub>2</sub> and NO<sub>x</sub> pollution and contributions of driving forces in urban areas in China, *Environ. Pollut.* 242 (2018) 239–248.
- [5] J. Zhang, C. Lian, W. Wang, et al., Amplified role of potential HONO sources in O<sub>3</sub> formation in North China Plain during autumn haze aggravating processes, *Atmos. Chem. Phys.* 22 (2022) 3275–3302.
- [6] Y.-C. Chan, M.J. Evans, P. He, et al., Heterogeneous nitrate production Mechanisms in intense haze events in the North China plain, *J. Geophys. Res. Atmos.* 126 (2021) e2021JD034688.
- [7] G. Geng, Y. Zheng, Q. Zhang, et al., Drivers of PM<sub>2.5</sub> air pollution deaths in China 2002–2017, *Nat. Geosci.* 14 (2021) 645–650.
- [8] M. Crippa, E. Solazzo, G. Huang, et al., High resolution temporal profiles in the

- emissions database for global atmospheric research, *Sci. Data* 7 (2020) 121.
- [9] Q. Zhang, Y. Zheng, D. Tong, et al., Drivers of improved PM<sub>2.5</sub> air quality in China from 2013 to 2017, *Proc. Natl. Acad. Sci. U.S.A.* 116 (2019) 24463–24469.
- [10] L. Tang, X. Xue, J. Qu, et al., Air pollution emissions from Chinese power plants based on the continuous emission monitoring systems network, *Sci. Data* 7 (2020) 325.
- [11] F. Liu, S. Beirle, Q. Zhang, et al., NO<sub>x</sub> lifetimes and emissions of cities and power plants in polluted background estimated by satellite observations, *Atmos. Chem. Phys.* 16 (2016) 5283–5298.
- [12] X. Li, J.B. Cohen, K. Qin, et al., Remotely sensed and surface measurement-derived mass-conserving inversion of daily NO<sub>x</sub> emissions and inferred combustion technologies in energy-rich northern China, *Atmos. Chem. Phys.* 23 (2023) 8001–8019.
- [13] B. Zheng, D. Tong, M. Li, et al., Trends in China's anthropogenic emissions since 2010 as the consequence of clean air actions, *Atmos. Chem. Phys.* 18 (2018) 14095–14111.
- [14] X. Bo, M. Jia, X. Xue, et al., Effect of strengthened standards on Chinese ironmaking and steelmaking emissions, *Nat. Sustain.* 4 (2021) 811–820.
- [15] J. Liu, D. Tong, Y. Zheng, et al., Carbon and air pollutant emissions from China's cement industry 1990–2015: trends, evolution of technologies, and drivers, *Atmos. Chem. Phys.* 21 (2021) 1627–1647.
- [16] Y. Zhang, Y. Zhao, M. Gao, et al., Air quality and health benefits from ultra-low emission control policy indicated by continuous emission monitoring: a case study in the Yangtze River Delta region, China, *Atmos. Chem. Phys.* 21 (2021) 6411–6430.
- [17] R. Wu, F. Liu, D. Tong, et al., Air quality and health benefits of China's emission control policies on coal-fired power plants during 2005–2020, *Environ. Res. Lett.* 14 (2019) 094016.
- [18] X. Lu, S. Zhang, J. Xing, et al., Progress of air pollution control in China and its challenges and opportunities in the ecological civilization era, *Engineering* 6 (2020) 1423–1431.
- [19] J. Cheng, D. Tong, Y. Liu, et al., Air quality and health benefits of China's current and upcoming clean air policies, *Faraday Discuss* 226 (2021) 584–606.
- [20] D. Tong, J. Cheng, Y. Liu, et al., Dynamic projection of anthropogenic emissions in China: methodology and 2015–2050 emission pathways under a range of socio-economic, climate policy, and pollution control scenarios, *Atmos. Chem. Phys.* 20 (2020) 5729–5757.
- [21] F. Liu, Q. Zhang, R.J. van der A, et al., Recent reduction in NO<sub>x</sub> emissions over China: synthesis of satellite observations and emission inventories, *Environ. Res. Lett.* 11 (2016) 114002.
- [22] J. Ha, M. Ayhan Kose, F. Ohnsorge, One-stop source: a global database of inflation, *J. Int. Money Finance* (2023) 102896.
- [23] A. Nikiforiadis, L. Mitropoulos, P. Kopelias, et al., Exploring mobility pattern changes between before, during and after COVID-19 lockdown periods for young adults, *Cities* 125 (2022) 103662.
- [24] Z. Liu, Z. Deng, G. He, et al., Challenges and opportunities for carbon neutrality in China, *Nat. Rev. Earth Environ.* 3 (2022) 141–155.
- [25] E. Solazzo, M. Crippa, D. Guizzardi, et al., Uncertainties in the emissions database for global atmospheric research (EDGAR) emission inventory of greenhouse gases, *Atmos. Chem. Phys.* 21 (2021) 5655–5683.
- [26] K. Qin, L. Lu, J. Liu, et al., Model-free daily inversion of NO<sub>x</sub> emissions using TROPOMI (MCMFE-NO<sub>x</sub>) and its uncertainty: declining regulated emissions and growth of new sources, *Rem. Sens. Environ.* 295 (2023).
- [27] C.R. Lonsdale, K. Sun, Nitrogen oxides emissions from selected cities in North America, Europe, and East Asia observed by the TROPospheric monitoring instrument (TROPOMI) before and after the COVID-19 pandemic, *Atmos. Chem. Phys.* 23 (2023) 8727–8748.
- [28] R.J. Pope, R. Kelly, E.A. Marais, et al., Exploiting satellite measurements to explore uncertainties in UK bottom-up NO<sub>x</sub> emission estimates, *Atmos. Chem. Phys.* 22 (2022) 4323–4338.
- [29] H. Kong, J. Lin, L. Chen, et al., Considerable unaccounted local sources of NO<sub>x</sub> emissions in China revealed from satellite, *Environ. Sci. Technol.* 56 (2022) 7131–7142.
- [30] S. Beirle, C. Borger, A. Jost, et al., Improved catalog of NO<sub>x</sub> point source emissions (version 2), *Earth Syst. Sci. Data* 15 (2023) 3051–3073.
- [31] A. Rey-Pommier, F. Chevallier, P. Ciais, et al., Quantifying NO<sub>x</sub> emissions in Egypt using TROPOMI observations, *Atmos. Chem. Phys.* 22 (2022) 11505–11527.
- [32] B. Zheng, Q. Zhang, G. Geng, et al., Changes in China's anthropogenic emissions and air quality during the COVID-19 pandemic in 2020, *Earth Syst. Sci. Data* 13 (2021) 2895–2907.
- [33] B. Zheng, G. Geng, P. Ciais, et al., Satellite-based estimates of decline and rebound in China's CO<sub>2</sub> emissions during COVID-19 pandemic, *Sci. Adv.* 6 (2020) eabd4998.
- [34] H. Li, B. Zheng, P. Ciais, et al., Satellite reveals a steep decline in China's CO<sub>2</sub> emissions in early 2022, *Sci. Adv.* 9 (2023) eadg7429.
- [35] J.P. Veefkind, I. Aben, K. McMullan, et al., TROPOMI on the ESA Sentinel-5 Precursor: a GMES mission for global observations of the atmospheric composition for climate, air quality and ozone layer applications, *Rem. Sens. Environ.* 120 (2012) 70–83.
- [36] J. van Geffen, H. Eskes, S. Compernelle, et al., Sentinel-5P TROPOMI NO<sub>2</sub> retrieval: impact of version v2.2 improvements and comparisons with OMI and ground-based data, *Atmos. Meas. Tech.* 15 (2022) 2037–2060.
- [37] K. Lange, A. Richter, A. Schönhardt, et al., Validation of Sentinel-5P TROPOMI tropospheric NO<sub>2</sub> products by comparison with NO<sub>2</sub> measurements from airborne imaging DOAS, ground-based stationary DOAS, and mobile car DOAS measurements during the S5P-VAL-DE-Ruhr campaign, *Atmos. Meas. Tech.* 16 (2023) 1357–1389.
- [38] N.A. Krotkov, L.N. Lamsal, E.A. Celarier, et al., The version 3 OMI NO<sub>2</sub> standard product, *Atmos. Meas. Tech.* 10 (2017) 3133–3149.
- [39] P.F. Levelt, G.H.J. Oord, M.R. Dobber, et al., The ozone monitoring instrument, *IEEE Trans. Geosci. Rem. Sens.* 44 (2006) 1093–1101.
- [40] H. Li, B. Zheng, TROPOMI NO<sub>2</sub> shows a fast recovery of China's economy in the first quarter of 2023, *Environ. Sci. Technol. Lett.* 10 (2023) 635–641.
- [41] F. Liu, A. Page, S.A. Strode, et al., Abrupt decline in tropospheric nitrogen dioxide over China after the outbreak of COVID-19, *Sci. Adv.* 6 (2020) eabc2992.
- [42] Y. Wu, S.J. Zhang, M.L. Li, et al., The challenge to NO<sub>x</sub> emission control for heavy-duty diesel vehicles in China, *Atmos. Chem. Phys.* 12 (2012) 9365–9379.
- [43] M. Cooper, R.V. Martin, A. Padmanabhan, et al., Comparing mass balance and adjoint methods for inverse modeling of nitrogen dioxide columns for global nitrogen oxide emissions, *J. Geophys. Res. Atmos.* 122 (2017) 4718–4734.
- [44] L.N. Lamsal, R.V. Martin, A. Padmanabhan, et al., Application of satellite observations for timely updates to global anthropogenic NO<sub>x</sub> emission inventories, *Geophys. Res. Lett.* 38 (2011).
- [45] M.M. Rienecker, M.J. Suarez, R. Gelaro, et al., MERRA: NASA's modern-era retrospective analysis for research and applications, *J. Clim.* 24 (2011) 3624–3648.
- [46] S. Peng, X. Lin, R.L. Thompson, et al., Wetland emission and atmospheric sink changes explain methane growth in 2020, *Nature* 612 (2022) 477–482.
- [47] Z. Liu, P. Ciais, Z. Deng, et al., Carbon Monitor, a near-real-time daily dataset of global CO<sub>2</sub> emission from fossil fuel and cement production, *Sci. Data* 7 (2020) 392.
- [48] S.J. Davis, Z. Liu, Z. Deng, et al., Emissions rebound from the COVID-19 pandemic, *Nat. Clim. Change* 12 (2022) 412–414.
- [49] L. Wang, X. Chen, Y. Zhang, et al., Switching to electric vehicles can lead to significant reductions of PM<sub>2.5</sub> and NO<sub>2</sub> across China, *One Earth* 4 (2021) 1037–1048.
- [50] L. Hao, H. Yin, J. Wang, et al., A multi-pronged approach to strengthen diesel vehicle emission monitoring, *Environ. Sci. Adv.* 1 (2022) 37–46.
- [51] Y. Tan, T. Wang, What caused ozone pollution during the 2022 Shanghai lockdown? Insights from ground and satellite observations, *Atmos. Chem. Phys.* 22 (2022) 14455–14466.
- [52] J. Cai, X. Deng, J. Yang, et al., Modeling transmission of SARS-CoV-2 Omicron in China, *Nat. Med.* 28 (2022) 1468–1475.
- [53] M.J. Cooper, R.V. Martin, M.S. Hammer, et al., Global fine-scale changes in ambient NO<sub>2</sub> during COVID-19 lockdowns, *Nature* 601 (2022) 380.
- [54] C. Wang, T. Wang, P. Wang, et al., Assessment of the performance of TROPOMI NO<sub>2</sub> and SO<sub>2</sub> data products in the North China plain: comparison, correction and application, *Rem. Sens.* 14 (2022).
- [55] K.F. Boersma, G.C.M. Vinken, H.J. Eskes, Representativeness errors in comparing chemistry transport and chemistry climate models with satellite UV–Vis tropospheric column retrievals, *Geosci. Model Dev. (GMD)* 9 (2016) 875–898.
- [56] V. Shah, D.J. Jacob, K. Li, et al., Effect of changing NO<sub>x</sub> lifetime on the seasonality and long-term trends of satellite-observed tropospheric NO<sub>2</sub> columns over China, *Atmos. Chem. Phys.* 20 (2020) 1483–1495.
- [57] L. Bindle, R.V. Martin, M.J. Cooper, et al., Grid-stretching capability for the GEOS-Chem 13.0.0 atmospheric chemistry model, *Geosci. Model Dev. (GMD)* 14 (2021) 5977–5997.
- [58] Y. Pang, Y. Li, Z. Feng, et al., Forest fire occurrence prediction in China based on machine learning methods, *Rem. Sens.* 14 (2022) 5546.
- [59] R. Xu, T. Ye, X. Yue, et al., Global population exposure to landscape fire air pollution from 2000 to 2019, *Nature* 621 (2023) 521–529.